2013 IEEE/RSJ International Conference on
Intelligent Robots and Systems (IROS)
November 3-7, 2013. Tokyo, Japan

Aerial Manipulation Using a Quadrotor with a Two DOF Robotic Arm

Suseong Kim[1], Seungwon Choi[2] and H. Jin Kim[3]

Abstract— **This paper presents aerial manipulation using a quadrotor with a two-DOF robot arm. By considering a quadrotor and robot arm as a combined system, the kinematic and dynamic models are developed, and an adaptive sliding mode controller is designed. With the controller, an autonomous flight experiment is conducted including picking up and delivering an object, which requires accurate control of a quadrotor and robot arm. Overall result shows that the proposed approach demonstrates satisfactory performance as a potential platform which can be utilized in various applications such as inspection, manipulation, or transportation in remote places.**

I. INTRODUCTION

Aerial robots that can hover and move around in three-dimensional Euclidean space are popular research platform. Due to their superior mobility, much interest is given to utilize them for mobile manipulation such as inspection of hard-to-reach structures or transportation in remote areas.

Previous research on aerial manipulation can be divided into three categories. The first approach is to install a gripper at the bottom of a UAV to hold a payload. In [2] and [3], a quadrotor with a gripper is used for transporting blocks and constructing structures. In [4], a team of quadrotors are employed for collaboratively picking up a relatively large object using a similar gripper. The stability of a helicopter with a gripper was investigated in [5]. The second approach is to suspend a payload with cables. In [6], an adaptive controller is presented to avoid swing excitation of a payload. Another approach for a similar problem can be found in [7], where the movement of a suspended payload is suppressed by trajectory optimization. In [8], specific attitude and position of a payload is achieved using cables connected to three quadrotors. In [9], the problem of carrying a payload under uncertainties such as strong wind is studied using single and multiple helicopters. The other types of research is concerned about interaction with existing structures, for example, for contact inspection. Research has been conducted on utilizing force a sensor [10] or a brush [11] as a manipulator. However, the above approaches have limitations for manipulation. In the first category using a gripper, payloads are rigidly connected to the body of an UAV. Accordingly, not only the attitude of the payload is restricted to the attitude of the UAV, but also the accessible range of the end effector is confined because of the UAV body and blades. In the second type using cables, the movement of the payload cannot be always regulated directly because manipulation is achieved using a cable which cannot always drive the motion of the payload as desired. The last cases are applicable to specialized missions such as wall inspection or applying normal force to a surface.

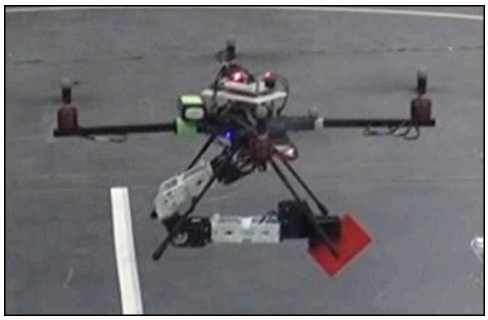

Fig. 1: Aerial manipulation using a quadrotor with 2DOF robotic arm

To cope with these limitations, one alternative approach is to equip an aerial vehicle with a robotic manipulator that can actively interact with the environment. For example, in [12], a testbed including four-DOF robot arms and a crane emulating an aerial robot is proposed. By combining the mobility of the aerial vehicle with the versatility of a robotic manipulator, the utility of mobile manipulation can be maximized.

When employing the robotic manipulator, the dynamics of the robotic manipulator is highly coupled with the aerial vehicle, which should be carefully considered in the controller design for the aerial vehicle. Also, an aerial robot needs to tolerate the reaction forces from the interactions with the object or external environment. These reaction forces may affect the stability of an aerial vehicle significantly.

Very few reports exist on handling the aerial vehicle and the robotic arms as an integrated system. Kinematic and dynamic models of the quadrotor combined with a multi-DOF robot arm are derived using the Euler-Lagrangian formalism in [13]. Based on that, simulation results using the Cartesian impedance control for the combined system is presented in [14]. In [16], effects of a manipulator on the quadrotor are simulated based on the dynamic model which considers a quadrotor and robotic arms separately, treating the arm as the disturbance to the quadrotor control loop. In [15], a quadrotor with light-weight manipulators are tested, although the movement of manipulators is not explicitly considered during the design of the PID controller.

This paper presents the design and experimental results of aerial manipulation using a quadrotor that has a two-DOF robotic manipulator attached. To utilize the combined

[1]Suseong Kim and Seungwon Choi are with the Department of Mechanical and Aerospace Engineering, Seoul National University, Seoul, South Korea suseongkim, cso103 at snu.ac.kr

[2]H. Jin Kim is with the Department of Mechanical and Aerospace Engineering, Seoul National University, Seoul, South Korea hjinkim at snu.ac.kr

system, a dynamics model which considers a quadrotor and a robotic manipulator as a unified system is presented. Also, an adaptive sliding mode controller is proposed to control the unified system. To verify the proposed approach, a hardware test result is presented, which involves picking up and delivering an object during autonomous flight.

This paper is organized as follows: In section II, the kinematic and dynamic models of a quadrotor with a two-DOF robotic manipulator attached are presented. Also, the adaptive sliding mode controller for the entire system is proposed. In section III, experimental setup and a mission scenario are described. Section IV presents experimental results and section V contains concluding remarks.

II. Kinematic and Dynamic Model

This section presents the kinematic and dynamic models of the quadrotor combined with a two-DOF manipulator. General version of deriving kinematics relations and dynamics equations for the similar combined system can be found in [13].

A. Kinematics for the Combined System

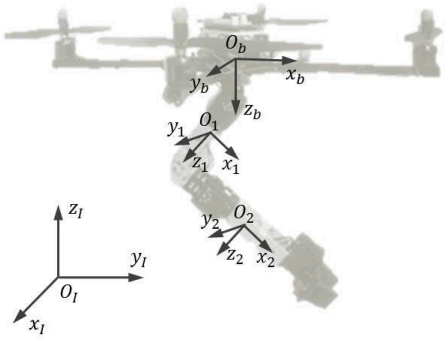

Fig. 2: Configuration of the coordinates for the combined system.

Fig. 2 shows the coordinate frames defined to derive the kinematic model of the combined system. The inertial coordinate frame is denoted as O_I, and O_b and O_i represent the body coordinate frames fixed to the quadrotor and links. The subscript $i = 1, 2$ denotes the link number. All body-fixed coordinate frames are located at the center of mass of their respective rigid bodies. The position of the center of mass of quadrotor in the inertial frame $p = [x\ y\ z]^T$, the Euler angles of the quadrotor $\Phi = [\phi\ \theta\ \psi]^T$ and the joint angles of the two-DOF manipulator $\eta = [\eta_1\ \eta_2]^T$ are chosen as the generalized coordinates. The joint angles η_1 and η_2 are defined about the positive y_b axis. The vector containing all the generalized coordinate variables is defined as

$$q = [p^T\ \ \Phi^T\ \ \eta^T]^T \tag{1}$$

The time derivative of p represents the translational velocity of the center of mass of the quadrotor, and the translational velocity in the body-fixed frame is denoted as $\dot{p}^b$. They are related by the rotation matrix $R_t \in SO(3)$ as

$$\dot{p} = R_t \dot{p}^b \tag{2}$$

The angular velocity of the quadrotor in the inertial and body fixed frame are defined as $\omega = [\omega_x\ \omega_y\ \omega_z]$ and $\omega^b = [\omega_x^b\ \omega_y^b\ \omega_z^b]$ respectively. ω and ω^b are also related by R_t. Also, the time derivative of the Euler angles $\dot{\Phi}$ can be mapped to ω by the transformation matrix T. The relations among $\dot{\Phi}$, ω and ω^b are

$$\omega = R_t \omega^b \tag{3}$$
$$\omega = T\dot{\Phi} \tag{4}$$
$$\omega^b = R_t^T T\dot{\Phi} = Q\dot{\Phi} \tag{5}$$

Let p_i^b be the position of the center of mass of link $i = 1, 2$ in the body-fixed frame O_b. Then, p_i, which is the position of the center of mass of the link i in the inertial frame O_I, is related to p_i^b by

$$p_i = p + R_t p_i^b \tag{6}$$

In addition, the translational and angular velocity of each manipulator link are related by the time derivative of the joint variables $\dot{\eta}$ and the Jacobian matrix $J_t \in \mathbb{R}^{2\times 2}$ and $J_r \in \mathbb{R}^{2\times 2}$ respectively.

$$\dot{p}_i^b = J_t \dot{\eta} \tag{7}$$
$$\omega_i^b = J_r \dot{\eta} \tag{8}$$

With equations (7) and (8), the translational and angular velocity of each link in the inertial frame are computed as

$$\dot{p}_i = \dot{p} + \dot{R}_t p_i^b + R_t \dot{p}_i^b \tag{9}$$
$$\dot{p}_i = \dot{p} + \widehat{\omega}_b R_t p_i^b + R_t J_t \dot{\eta} \tag{10}$$
$$\omega_i = \omega + R_t J_r \dot{\eta} \tag{11}$$

For simplicity, equations (2),(4),(9) and (10) are rewritten in the following matrix form.

$$\dot{p} = [I_{3\times 3}\ \ 0_{3\times 3}\ \ 0_{3\times 2}]\dot{q} = M_{t,b}\dot{q} \tag{12}$$
$$\omega = [0_{3\times 3}\ \ T\ \ 0_{3\times 2}]\dot{q} = M_{r,b}\dot{q} \tag{13}$$
$$\dot{p}_i = [I_{3\times 3}\ -(R_t p_i^b)^\wedge T\ \ R_t J_{t,i}]\dot{q} = M_{t,i}\dot{q} \tag{14}$$
$$\omega_i = [0_{3\times 3}\ \ T\ \ R_t J_{r,i}]\dot{q} = M_{r,i}\dot{q} \tag{15}$$

where the subscript $\cdot \times \cdot$ represents the size of I and 0. Also, $^\wedge$ is the operator that converts a vector into a skew-symmetric matrix. With the above relations, the time derivative of the generalized coordinate variable vector $\dot{q}$ is easily mapped into the translational and angular velocities of the quadrotor and each link in the inertial coordinate frame.

B. Dynamics Derivation for Combined System

To derive the dynamics of the combined system, the Lagrange-D'Alembert equation is used.

$$\frac{d}{dt}\frac{\partial \mathcal{L}}{\partial \dot{q}} - \frac{\partial \mathcal{L}}{\partial q} = \tau + \tau_{ext} \tag{16}$$

$$\mathcal{L} = \mathcal{K} - \mathcal{U} \tag{17}$$

where $\mathcal{K}$ and $\mathcal{U}$ are the total kinetic and potential energy of the combined system and τ represents the generalized force. τ_{ext} indicates external disturbance applied to the system.

The total kinetic energy is the sum of the kinetic energy of individual components, which are the quadrotor and two links. The total kinetic energy $\mathcal{K}$ and its components are as follows:

$$\mathcal{K} = \mathcal{K}_b + \sum_{i=1}^{2} \mathcal{K}_i \quad (18)$$

$$\mathcal{K}_b = \frac{1}{2}\dot{p}^T m_b \dot{p} + \frac{1}{2}\dot{\Phi}^T T^T R_t I_b R_t^T T \dot{\Phi} \quad (19)$$

$$\mathcal{K}_i = \frac{1}{2}\dot{p}_i^T m_i \dot{p}_i + \frac{1}{2}\omega_i^T (R_t R_i) I_i (R_t R_i)^T \omega_i \quad (20)$$

where m is the mass and I is the inertia matrix. The subscripts b and i indicate the corresponding values are with respect to O_b and O_i respectively.

Likewise, the total potential energy is the sum of potential energy of each component. The total potential energy $\mathcal{U}$ and its components are described by the equations below:

$$\mathcal{U} = m_b g e_3^T p + \sum_{i=1}^{2} m_i g e_3^T (p + R_t p_i^b) \quad (21)$$

where the first and last terms are the potential energies of the quadrotor and link i, respectively. e_3 is the unit vector $[0\ \ 0\ \ 1]^T$ and g is the gravity.

By substituting equations (17),(18) and (21) in equation (16), the dynamics equation which includes all components as one system can be derived as the following

$$M(q)\ddot{q} + C(q,\dot{q})\dot{q} + G(q) = \tau + \tau_{ext} \quad (22)$$

where $M(q) \in \mathbb{R}^{8\times 8}$ is the inertia matrix which is positive definite and symmetric. $C(q,\dot{q})$ is the Coriolis matrix and $C(q,\dot{q})\dot{q}$ represents the Coriolis and centrifugal force terms. In addition, $G(q)$ includes gravity effects at each joint [1]. The total kinetic energy can be calculated using the inertia matrix $M(q)$ as

$$\mathcal{K} = \frac{1}{2}\dot{q}^T M(q)\dot{q} \quad (23)$$

By substituting equations (12), (13), (14) and (15) into equation (23), the inertia matrix $M(q)$ is computed as the following equation.

$$M(q) = M_{t,b}^T m_b M_{t,b} + M_{r,b}^T R_t I_b R_t^T M_{r,b} + \sum_{i=1}^{2} M_{t,i}^T m_i M_{t,i} + M_{r,i}^T (R_t R_i) I_i (R_t R_i)_t^T M_{r,i} \quad (24)$$

where R_i is the coordinate transformation matrix from link i of the manipulator to the quadrotor body-fixed coordinate. The Coriolis matrix $C(q,\dot{q})$ can be derived by calculating each element with the following relation [1].

$$c_{kj} = \sum_{i=1}^{8} \frac{1}{2}\left\{ \frac{\partial m_{kj}}{\partial q_i} + \frac{\partial m_{ki}}{\partial q_j} - \frac{\partial m_{ij}}{\partial q_k} \right\}$$

where $m_{\alpha\beta}$ indicates the element $\alpha\beta$ of the inertia matrix $M(q)$. $G(q)$ is calculated with the following partial derivative

$$G(q) = \frac{\partial \mathcal{U}}{\partial q} \quad (25)$$

Generalized torque related to the joint variable η can be actuated directly through joint actuators, such as servo motors. However, the generalized torque corresponding to p and Φ need to be transformed to be usable as the quadrotor input. The actual quadrotor inputs are given in the PWM signals to motors, and those signals are mixed to generate thrust or torques. But for the description in this paper, we can treat the input to the quadrotor as the following four values: F, the total thrust value of the four propellers of the quadrotor, and τ_x, τ_y and τ_z, the torque values applied to the quadrotor body coordinate in x, y and z direction, respectively.

Later, in section II.C, an adaptive sliding mode controller will be described to design the τ. Then the computed control signal τ can be converted to the input values of the quadrotor and joint actuators. Let $\tau_\eta \in \mathbb{R}^{2\times 1}$ denote the joint torque values of the manipulator, and the numbers in parenthesis indicate the element in the corresponding matrix or vector. Then,

$$\begin{bmatrix} F \\ \tau_x \\ \tau_y \\ \tau_z \\ \tau_\eta \end{bmatrix} = \begin{bmatrix} R_t(3,3) & 0 & 0 \\ 0 & Q^{-1} & 0 \\ 0 & 0 & I_{2\times 2} \end{bmatrix}^{-1} \begin{bmatrix} \tau(3) \\ \vdots \\ \tau(8) \end{bmatrix} \quad (26)$$

The other two elements of τ, i.e. $\tau(1)$ and $\tau(2)$, are modulated to the desired ϕ_d and θ_d of a quadrotor as

$$\begin{bmatrix} \theta_d \\ \phi_d \end{bmatrix} = \frac{1}{F}\begin{bmatrix} \cos\psi & \sin\psi \\ \sin\psi & -\cos\psi \end{bmatrix}\begin{bmatrix} \tau(1) \\ \tau(2) \end{bmatrix} \quad (27)$$

This relation is derived based on the small roll and pitch angle assumption.

C. Adaptive Sliding Mode Controller

This subsection describes the control design of the combined system (22). In this research, aerial manipulation includes motions involving both picking and releasing an object during hovering flight. Position holding, one of the most important functions for accurate manipulation, can be significantly disturbed by a sudden quadrotor attitude change due to the additional torque caused by grabbing or releasing an object. In other words, robustness of the controller is a key issue for using the aerial vehicle to manipulate an object as desired. Also, the controller should be able to handle problems such as battery drains, miscalculated mechanical properties, measurement bias or noise. To cope with these uncertainties, the controller needs to be adaptive. In this paper, to control the combined system, an adaptive sliding mode controller is used.

To design a controller for equation (22), the error e and sliding surface s are defined as the following:

$$e = q - q_d \quad (28)$$

$$s = \dot{e} - \Lambda e \quad (29)$$

$$\dot{q}_r = \dot{q} - s = \dot{q}_d - \Lambda e \quad (30)$$

where λ is a positive diagonal matrix. With these definitions, the proposed control law for τ is

$$\tau = \hat{M}\ddot{q}_r + \hat{C}\dot{q}_r + \hat{G} + \hat{\Delta} - As - K\mathbf{sgn}(s) \quad (31)$$

Here, $\hat{M}$, $\hat{C}$ and $\hat{G}$ represent the estimation of each matrix. A and K are positive gain matrices. Also, $\hat{\Delta}$ describes the estimated uncertainty. By substituting the proposed control law to the dynamics equation (22), we can derive the following relations:

$$M\dot{s} + Cs + As = -\Delta + \hat{\Delta} - K\mathbf{sgn}(s) + \tau_{ext} \quad (32)$$

$$M\dot{s} + (C + A)s = \tilde{\Delta} - K\mathbf{sgn}(s) + \tau_{ext} \quad (33)$$

where

$$\Delta = -\tilde{M}\ddot{q}_r - \tilde{C}\dot{q}_r - \tilde{G} \quad (34)$$

and $\tilde{}$ indicates the estimation error of the corresponding matrices and vectors. With these equations, stability analysis can be performed as the following.

Proof. Let a Lyapunov candidate function be

$$V = \frac{1}{2}s^T Ms + \frac{1}{2}\tilde{\Delta}^T\tilde{\Delta} > 0 \quad (35)$$

with directional time derivative

$$\dot{V} = \frac{1}{2}s^T\dot{M}s + s^T M\dot{s} + \tilde{\Delta}^T\dot{\tilde{\Delta}} \quad (36)$$

$$= s^T(-As + \tilde{\Delta} - K\mathbf{sgn}(s) + \tau_{ext}) + \tilde{\Delta}^T\dot{\tilde{\Delta}} \quad (37)$$

$$= -s^T As - s^T(K\mathbf{sgn}(s) - \tau_{ext}) + \tilde{\Delta}^T(s + \dot{\tilde{\Delta}}) \quad (38)$$

$$= -s^T As - s^T(K\mathbf{sgn}(s) - \tau_{ext}) \quad (39)$$

$$< 0$$

In the derivation, skew symmetricity of $\dot{M} - 2C$ is used. Negative definitiveness of equation (39) can be satisfied with arbitrarily large matrices A and K.

In equation (38), it is assumed that $s + \dot{\tilde{\Delta}} = 0$. From this relation, the following adaptation law can be derived.

$$\dot{\hat{\Delta}} - \dot{\Delta} = -s \quad (40)$$

with the assumption that Δ changes very slow compared with the adaptation rate

$$\dot{\hat{\Delta}} = -s \quad (41)$$

As a result, by integrating $-s$, estimation of the uncertainty $\hat{\Delta}$ can be computed.

III. Experimental Setup

A. Hardware setup

The quadrotor used in this paper is a Smart Xcopter [20] whose arm length is 25cm and weight is approximately 0.9 kg. The carrying capacity of the quadrotor is about 0.45 kg. To transmit the control signal to the quadrotor, Spectrum DX7 transmitters is connected to the ground station through Endurance R/C PCTx. The robotic arm is customized with a Bioloid frame set and Dynamixel MX-28 servomotors [18]. The shape of each link is shown in fig. 3. The length of the arm when it is fully stretched is 0.32 meter and the total weigh is about 0.370 kg. The ground station and robot arm communicate via bluetooth. To grab a small object, a parallel gripper connected with an AX-12 servomotor is used [17]. Also, each servomotor has an encoder which measures joint angles. Vicon [19], an indoor GPS system, is used to estimate

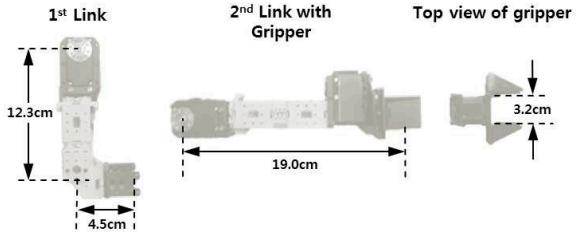

Fig. 3: Specification of each link of the robotic manipulator

the position and attitude of the quadrotor. With this device, the estimated position, attitude and their derivatives are computed up to 100Hz. Measured quadrotor and joint states are used in the adaptive sliding mode controller. The desired configuration q_d is obtained by solving inverse kinematics with the known position of the object for grasping and releasing.

Overall hardware configuration is summarized in fig. 4.

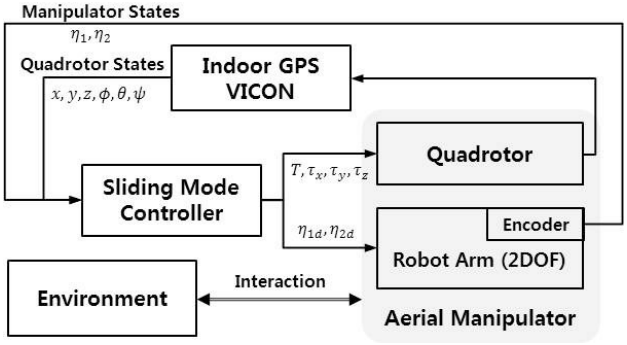

Fig. 4: Configuration of the overall system.

B. Mission Scenario

To emphasize the capability of aerial manipulation with a two-DOF robot manipulator over using an gripper or cable, an experimental scenario is devised.

After taking off, the quadrotor moves to an object. It is assumed that the position of the object is known in advance (measured by Vicon beforehand in this case), which will soon be relaxed using vision. Once the quadrotor arrives at the designated position, the robotic arm moves to the position of the object and grabs it.

While grabbing the object, the quadrotor moves to the next place to reach where the object is laid down. When the quadrotor gets close enough to the designated location, the robotic arm manipulates the object to release it at the desired position. Here, the releasing point is located inside of a shelf

where only a two or higher DOF robot arm can reach. After completing the above missions, the quadrotor goes back to the place where it took off and lands.

IV. Results

The proposed aerial manipulation using the adaptive sliding mode controller is validated by an experiment. The results are summarized in figs. 5-9.

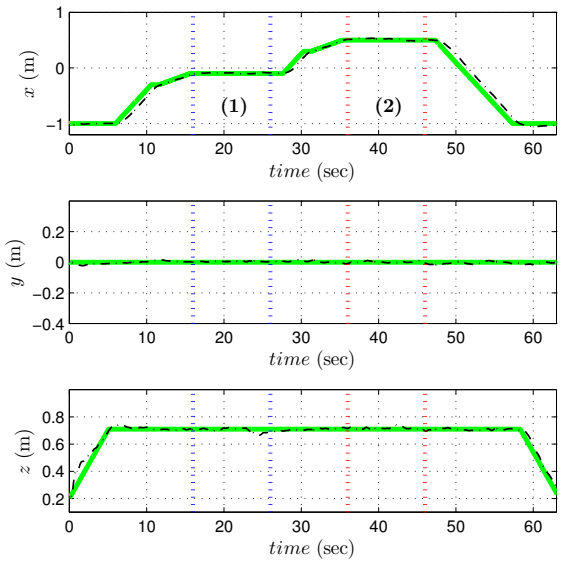

Fig. 5: Position history of the quadrotor. Solid-green line is the desired position and dashed-black line is the measured position. (1): pick-up phase, (2): release phase

The first mission for the combined system is picking up an object. The object used in the experiment is an wood block of demension $(H)7.5 \times (D)5 \times (W)1.5$ cm. Given that the gap of the end effector is only 3.2 cm, it is clear that grabbing the wood block requires accurate control of the quadrotor and robot arm concurrently. It is shown in figs. 5-7 that quadrotor position and attitude, and manipulator's position follow the reference trajectory precisely during the pick-up phase. Even though no information such as mass and moment of inertia about the wood block is given to the adaptive sliding mode controller, overall manipulation is successful because of robustness of the sliding mode controller. During the pick-up phase, root-mean-square error of the quadrotor position is only 2.08 cm. In fig. 8, a sequence of images taken in the pick-up task is shown.

The second mission is releasing the wood block inside a shelf. The size of the gap of shelf is about $(H)16 \times (W)22cm$. To lay the wood block down inside the shelf, most part of the second link with gripper needs to be put into the shelf. Again, given the size of the second link with respect to the size of the shelf, it is a difficult task that demands exact control of the combined system. As shown in fig. 9, the task is smoothly completed. In the release phase, root-mean-square error of the quadrotor is 2.56 cm.

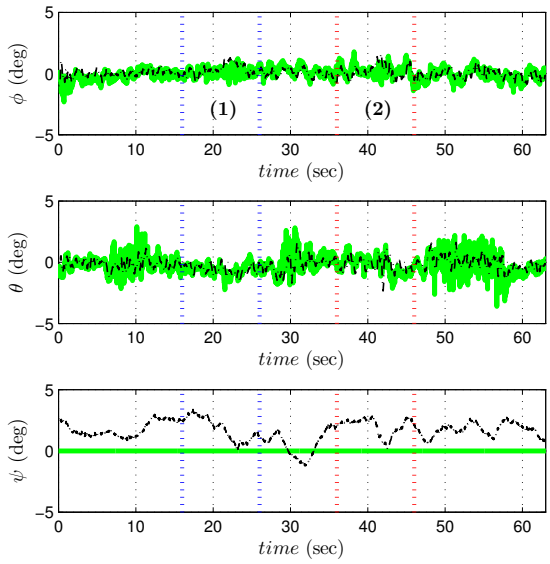

Fig. 6: Attitude history of the quadrotor. Solid-green line is the desired attitude and dashed-black line is the measured attitude. (1): pick-up phase, (2): release phase

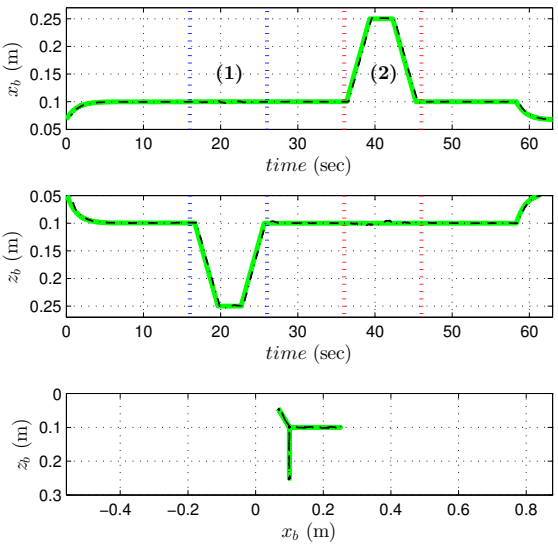

Fig. 7: End effector position history in the quadrotor body fixed frame. The third figure is plotted for full flight duration. Solid-green line is the desired position and dashed-black line is the measured positionm (1): pick-up phase, (2): release phase

From the entire trajectory histories in figs. 5-7, it is shown that the quadrotor and robotic arm are controlled as desired during the full flight including manipulations of an object. These results also means that the provided approach can be utilized in expanded ma-

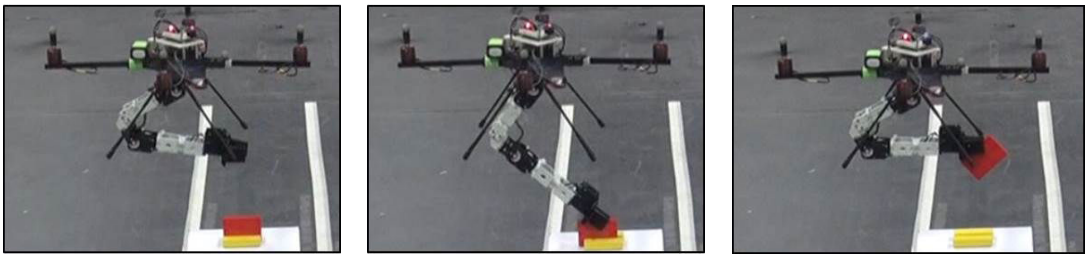

(a) Quadrotor is approaching the designated position

(b) Robot arm is grabbing the wood block

(c) The wood block is picked up and quadrotor moves to the next position

Fig. 8: Pictures taken during pick-up phase

(a) Quadrotor is approaching the designated position

(b) The robot arm is releasing the wood block at the desired spot

(c) Robot arm is retreating to go back to the origin position

Fig. 9: Pictures taken during release phase

nipulation and transportation applications. A video clip of the experiment is posted on the following URL: http://icsl.snu.ac.kr/video/iros2013/aerialManipulation.mp4.

V. Conclusion

This paper presents a successful application of a quadrotor with a two-DOF robot arm attached for picking up and delivering an object. Kinematic and dynamic models for the combined system are analysed and an adaptive sliding mode controller is designed to control them all together. This is demonstrated in an experiment with a scenario consisting of picking up an object, moving, and releasing it inside of a shelf. The experimental results demonstrates satisfactory performance to perform the designed tasks.

ACKNOWLEDGMENT

This work was supported by the National Research Foundation of Korea(NRF) grant funded by the Korea government(MEST)(No. 20110001276, 2013013911).

References

[1] R. M. Murray, Z.Li, and S. S. Sastry, A Mathematical Introduction to Robotic Manipulation. Boca Raton, FL: CRC, 1994.

[2] Q. Lindsey, D. Mellinger, and V. Kumar, "Construction of cubic structures with quadrotor teams," in Proc. Robotics: Science and Systems (RSS), Los Angeles, CA, June 2011.

[3] J. Willmann, F. Augugliaro, T. Cadalbert, R. DAndrea, F. Gramazio, and M. Kohler, "Aerial robotic construction towards a new field of architectural research," International Journal of Architectural Computing, 10(3), pp. 439-460, Sep. 2012.

[4] D. Mellinger, M. Shomin, N. Michael, and V. Kumar, "Cooperative grasping and transport using multiple quadrotors," Distributed Autonomous Robotic Systems, 2010, 545-558

[5] P. Pounds, D. Bersak, and A. Dollar Grasp from the air: hovering capture and load stability, IEEE/RSJ International Conference on Intelligent Robots and Systems 2011, San Francisco, CA Sep 2011.

[6] M. Bisgaard, A. la Cour-Harbo, and J. Bendtsen, "Adaptive control system for autonomous helicopter slung load operations," Control Engineering Practice, vol. 18, no. 7, pp. 800811, 2010.

[7] I. Palunko, R. Fierro, and P. Cruz, "Trajectory generation for swing-free maneuvers of a quadrotor with suspended payload: A dynamic programming approach," in IEEE International Conference on Robotics and Automation, pp. 2691-2697, May 2012.

[8] N. Michael, J. Fink and V. Kumar, "Cooperative manipulation and transportation with aerial robots," Autonomous Robots, 30(1), pp. 73-86, 2011.

[9] M. Bernard, K. Kondak, I. Maza, and A. Ollero, "Autonomous transportation and deployment with aerial robots for search and rescue missions," Journal of Field Robotics, vol. 28, no. 6, pp. 914931, 2011.

[10] A. Torrem, D. Mengoli, R. Naldi, F. Forte, A. Macchelli, and L. Marconi, "A prototype of aerial manipulator," IEEE/RSJ International Conference on Intelligent Robots and Systems, Algarve, Portugal, pp. 2653-2654, Oct 2012.

[11] A. Albers, S. Tautmann, T. Joward, T. A. Nguyen, M. Frietsch, and C. Sauter, "Semi-autonomous flying robot for physical interaction with environment," IEEE conference on Robotics Automation and Mechatronics, pp. 441-446, 2010.

[12] C. M. Korpela, T. W. Danko, and P. Y. Oh, "MM-UAV:Mobile manipulating unmanned aerial vehicle," Journal of Intelligent and Robotic Systems, 1-9, 2012.

[13] V. Lippiello and F. Ruggiero, "Cartesian impedance control of a UAV with a robotic arm," in 10th International IFAC Symposium on Robot Control, Dubrovnik, Croatia, Sep 2012.

[14] V. Lippiello and F. Ruggiero, "Exploiting redundancy in Cartesian impedance control of UAVs equipped with a robotic arm," IEEE/RSJ International Conference on Intelligent Robots and Systems, Vilamoura, Portugal, Oct 2012.

[15] M. Orsag, C. Korpela, P. Oh, "Modeling and control of MM-UAV: Mobile manipulating unmanned aerial vehicle," J Intell Robot System, pp. 227-240, 2013.

[16] M. Orsag, "Mobile manipulating unmanned aerial vehicle(MM-UAV): Towards aerial manipulators," System, 13, 14

[17] Gripper, http://www.trossenrobotics.com/p/phantomx-parallel-ax12-gripper.aspx

[18] Bioloid Frame and Dynamixel, http://www.robotis.com/xe

[19] VICON, http://www.vicon.com

[20] Smart Xcopter, http://www.xcopter.com